Journal of Polymers and the Environment (2023) 31:5446–5461
https://doi.org/10.1007/s10924-023-02949-0

ORIGINAL PAPER

Pentaerythritol and Glycerol Esters Derived from Gum Rosin as Bio-Based Additives for the Improvement of Processability and Thermal Stability of Polylactic Acid

Harrison de la Rosa-Ramírez[1] · Franco Dominici[2] · José Miguel Ferri[1] · Francesca Luzi[3] · Debora Puglia[2] · Luigi Torre[2] · Juan López-Martínez[1] · María Dolores Samper[1]

Accepted: 31 May 2023 / Published online: 4 July 2023

Abstract

Gum rosin esters are some of the most common gum rosin derivatives used in different applications, such as coatings, paper, varnishes, chewing gum, and food industries. In this study, gum rosin esters are used as additives for polylactic acid (PLA) to improve its processability and thermal stability. Blends of an amorphous PLA with two different gum rosin esters, pentaerythritol ester and glycerol ester, were prepared by melt extrusion process in concentrations from 1, 3, and 5 phr. Besides the comparison of thermal degradation, microstructure assessment, and melt flow index (MFI) analysis, the processability performance during testing samples production by injection molding process was evaluated. Experimental results showed that MFI values of PLA-gum rosin ester blends increased by 100%, 147%, and 164%, along with increasing content of gum rosin esters addition, in both cases. Also, both derivatives slightly improved PLA thermal stability (around 3ºC higher). Injection molding temperature decreased by at least 20 °C for PLA-gum rosin ester blends compared with neat PLA. Furthermore, the maximum tensile strength of PLA-gum rosin esters was negligibly affected in formulations with low content of gum rosin esters, and the FESEM images revealed a good dispersion and compatibility of gum rosin ester particles into PLA matrix in both concentrations.

Keywords Gum rosin esters · Gum rosin · Bio-based polymer · Polylactic acid processability

Introduction

Conventional polymers, such as polyethylene (PE), ethylene vinyl acetate (EVA), and acrylonitrile butadiene styrene (ABS), among others, are considered easily processable polymers [1–4]. Meanwhile, other conventional polymers, such as polyvinyl chloride (PVC) and polyethylene terephthalate (PET), are considered as polymers of difficult processability. In the case of PVC, the processability could be problematic due to the high molecular rigidity caused by the cohesive bonds produced by the dipole moments between the chlorine atoms, which are of high electronegativity and volume, giving rise to an amorphous polymer without the ability to crystallize. In addition, PVC is a thermally unstable polymer, susceptible to thermal degradation, which generates hydrochloric acid [5, 6]. This is a gas toxic to humans by inhalation and highly corrosive to machinery [7]. In the case of PET, the processability problems are related to its viscosity in molten state, which leads to the use of temperatures above its melting point to facilitate fluidity [8]. In the biopolymers classification, polymers with processability drawbacks, such as polyhydroxybutyrate (PHB) and poly lactic acid (PLA) can also be found. PHB exhibits thermal instability above its melting temperature, which makes it susceptible to thermal degradation when processed [9, 10]. PLA, which it is investigated in the present work,

✉ Harrison de la Rosa-Ramírez
hardela@epsa.upv.es; harrison.dr@hotmail.com

[1] Instituto de Tecnología de Materiales (ITM), Universitat Politècnica de València (UPV), Plaza Ferrándiz y Carbonell 1, Alcoy, Alicante 03801, Spain

[2] Civil and Environmental Engineering Department, University of Perugia, Strada di Pentima 4, Terni 05100, Italy

[3] Department of Materials, Environmental Sciences and Urban Planning (SIMAU), Polytechnic University of Marche, Via Brecce Bianche 12, Ancona 60131, Italy

is an aliphatic polyester obtained through different methods, including direct polymerization of lactic acid at temperatures above 120 °C. It possesses relatively high tensile strength, good transparency, and barrier properties. In addition, PLA is a promising biodegradable polymer widely used in different sectors, such as agriculture, [11, 12] food packaging, [13, 14] and medical and pharmaceutical industries, due to its biocompatibility characteristics, that makes it suitable for biomedical applications [15–17]. However, despite possessing attractive properties and good characteristics as a compostable biopolymer, the high melt viscosity of PLA represents a drawback for additive manufacturing processes, if compared with ABS [18]. Moreover, its high rigidity is a limitation that prevents good processability by methods such as blown film extrusion [19, 20].

Due to the difficulties of processability shown by PLA, and the need of adapting it to various processing methods, different works have been conducted in order to provide an efficient solution. Those works include reactive extrusion and melt blending with various biopolymers and chain extender component [21, 22]: the use of additives that improve its properties, performance and processability is also increasing. Generally, these additives consist of substances that act as lubricants (internal or external), plasticizers (mostly phthalic anhydride esters), fillers and heat stabilizers, e.g., organometallic compounds; tin (Sn), lead (Pb), Zinc (Zn), etc., [23, 24]. Part of the disadvantages of these additives, especially plasticizers and lubricants, is that they are synthetic-based chemical compounds, in addition to their easy migration drawbacks.

To this effect, the study and research of natural bio-based additives that can modify and enhance polymeric material properties and processability is highly interesting for industry and academia [25–27]. Although these natural origin additives are extended to conventional polymers, they are mainly used in biopolymers, aiming to keep the eco-friendly and bio-based commitment of these biopolymers. Some natural additives of the most significant research interest are fatty esters, oils (maleinized and epoxidized), and vegetable extracts of different compositions such as rosin resins [28–31]. In our previous work, gum rosin (molecular weight, 302 g/mol) and a pentaerythritol ester of gum rosin of low molecular weight (1469 g/mol) were used to study the modification of PLA mechanical performance and hydrophobicity [32] due to being abundant resources of renewable origin and eco-friendly substances already used as food additive [33], and as microencapsulation in pharmaceutical applications [34]. The material preparation was done by melt extrusion. As well, both rosin derivatives were used for the development and improvement of polybutylene adipate terephthalate (PBAT)-rosin blends performance for injection molded materials [35].

In this work, the research aim is focused on the development of a novel PLA-gum rosin ester blend using two gum rosin esters of higher thermal stability and tackifier behavior than those used in the previous study. Those improvements in gum rosin esters make them suitable as multifunctional additives for the coating material, rubber production, and oil-based lubricant and enhance thermoplastic road-making paints [36–39]. Therefore, noticing the suitability of those gum rosin esters as multifunctional additives, pentaerythritol ester of gum rosin of high molecular weight (2074 g/mol) and a glycerol ester of gum rosin were melt-compounded with PLA polymer matrix in concentrations of 1, 3, and 5 parts per hundred resins (phr) by extrusion method to evaluate its performance. The evaluation of their processability by injection molding, compared with the materials behavior under MFI analysis was carried out. Additional techniques for characterization, such as thermal degradation analysis, mechanical test, microstructure assessment and FTIR analysis were conducted as evaluation and quality control methods on the resulting materials.

Experimental

Materials

A commercial grade of biodegradable polylactic acid (PLA) Purapol LX-175, supplied by Corbion Purac (Amsterdam, Netherlands) was used to prepare the blends. This PLA contains 4% of D-isomer, its melt flow index (MFI) is on the range of 3–5 g/10 min (190 °C, 2.16 kg) and its density is 1.24 g cm^{-3}. For the binary compound formulations, two gum rosin esters were used as additives: UTP120, a pentaerythritol ester of gum rosin (labeled as UTP, with softening point between 110 and 115 °C and maximum acid value of 15) and UTG88, a glycerol ester of gum rosin (labeled as UTG, with softening point between 86 and 90 °C and maximum acid value of 15). Figure 1 depicts the typical molecular structures of modified rosin products after esterification [40–43]. Both gum rosin esters were kindly supplied by United Resins. Produção de Resinas S. A (Figueira da Foz, Portugal).

Preparation of the Binary Blends

Prior to processing, UTP and UTG gum rosin esters were cracked into small fragments using a porcelain mortar. Then, they were sifted in a RP09 CISA® (Barcelona, Spain) sieve shaker to be used in grain form (particle size between 3 and 5 mm). The gum rosin esters (in grain form) were blended with PLA in concentrations of 1, 3 and 5 parts per

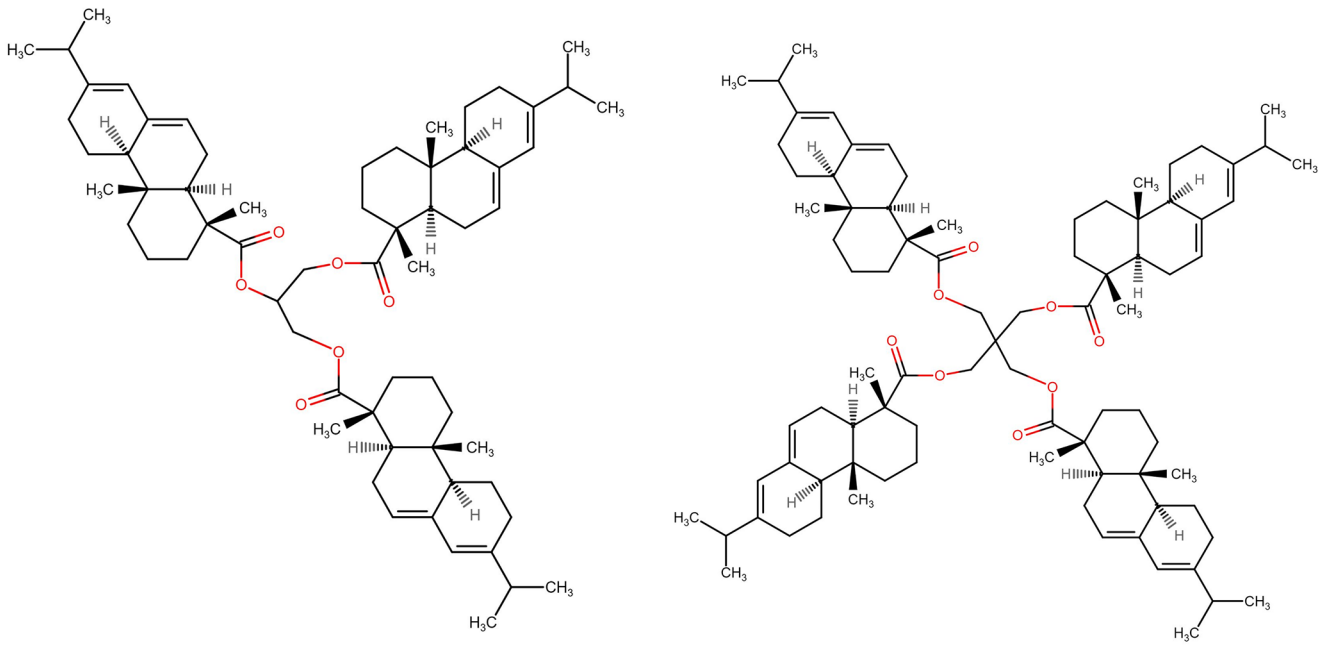

Fig. 1 Molecular structures of modified rosin products after esterification

Table 1 Composition and coding of neat PLA and PLA with different amount of UTP and UTG.

Code for UTP	Code for UTG	Resin content (phr)
PLA		-
PLA-1UTP	PLA-1UTG	1
PLA-3UTP	PLA-3UTG	3
PLA-5UTP	PLA-5UTG	5

hundred resins (phr). The formulations coding is indicated in Table 1.

Before processing the formulations, PLA pellets and the gum rosin esters (UTP and UTG) were subjected to a drying process at 50 °C for 12 h in a dehumidifier oven model D-82,152 from MMM Medcenter GmbH (München, Germany) to reduce the residual moisture. Subsequently, materials were premixed in plastic bags by manual agitation according to each formulation prepared. After that, the premixed formulated materials were dosed by a K-QX2 single-screw gravimetric feeder, from K-Tron GmbH (Niederlenz, Switzerland), into a compounder twin-screw extruder, with a length-to-diameter ratio of 25 mm (L/D), from Haake Rheocord 9000 system torque (Karlsruhe, Germany) with a temperature profile of 60/160/165/170/175/180/180°C from the feed hopper to the material outlet nozzle, at a screw speed of 20 rpm. Following, the melt-blended materials were injected-molded in standard test specimens for characterization in a Meteor 270/75 injection machine from Mateu-&-Solé (Barcelona, Spain). The injection molding parameters were settled as shown in Table 2, obtaining dumbbell and rectangular testing specimens according to ISO 527-2 [44] and ISO 179-1 [45].

Table 2 Injection molding parameters of PLA and PLA-gum rosin ester blends

Injection molding parameters	*Samples*						
	PLA	PLA-1UTP	PLA-3UTP	PLA-5UTP	PLA-1UTG	PLA-3UTG	PLA-5UTG
Injection temperature (°C)	180	160	160	160	160	160	160
Injection rate (cm^3/s)	20	15	15	10	15	10	10
Injection pressure (Bar)	110	70–80	70–80	70–80	70–80	70–80	70–80
Packing pressure (Bar)	105	65	65	65	65	65	65
Packing time (s)	25	14	14	14	14	14	14
Dosing volume (cm^3)	35	45	45	45	45	45	45

Techniques for Characterization

Infrared Spectroscopy (FTIR)

Fourier transform infrared (FTIR) spectra were recorded in the wave number region between 4000 and 600 cm^{-1} (118 scans, at 4 cm^{-1} resolution) over injected-molded pieces by ATR mode, in a JASCO 615 plus spectrometer (Easton, MD, USA). Tests measurements were overwritten in a background spectrum, previously recorded to compensate the moisture effect and presence of carbon dioxide in the air.

Melt Flow Index Analysis

The melt flow index (MFI) determination was performed under the guidelines of ISO 1133 [46], at a die temperature of 190 °C with a fixed nominal load of 2.16 Kg, using an Melt flow indexer Mod. 452 from MP Strumentti (Bussero, Italy) equipped with a standard die of 2 mm diameter in nozzle and 8 mm in length.

Thermal Analysis and Thermomechanical Characterization

Thermogravimetric analyses (TGA) and differential scanning calorimetry (DSC) tests were performed as evaluation analyses. The tests were carried out to assesses the effect of gum rosin esters derivatives (UTP and UTG) over the thermal stability and main thermal phase transitions of the PLA binary melt-blended formulations, i.e., changes from the vitreous to the rubbery state, crystallization behavior, and melting point; throughout the determination of the glass transition temperature (T_g), cold crystallization temperature (T_{cc}) and melting temperature (T_m), respectively.

The thermal stability was determined using a TGA equipment model PT1000 from Linseis Inc. (Selb, Germany), by monitoring the weight changes of initial mass samples (15–18 mg), running a dynamic heating cycle from 30 to 700 °C, at a constant heating rate of 10 °C/min in presence of nitrogen atmosphere (30 mL min^{-}). The initial thermal decomposition ($T_{5\%}$) of the samples were determined at 5% of their mass loss, whereas the temperatures of the maximum degradation rate (T_{max}) were obtained from the corresponding peak of the first derivative of the TGA curves (DTG).

DSC tests were carried out in a Q200 calorimeter from TA Instruments (New Castle, USA). Samples (mass range of 7–10 mg) placed in sealed standard aluminum crucibles (40 µl) were subjected to a dynamic thermal program with a heating/cooling ramp of 10 °C min^{-1}, settled in three steps: (i) heated from 30 to 190 °C, (ii) a cooling step from 190 to -30 °C, and (iii) a reheat step up to 200 °C in presence of nitrogen atmosphere (stream-rate 30 mL min^{-1}).The degree crystallinity (X_c) of PLA and PLA-gum rosin ester blends, were calculated using the following Eq. 1:

$$\boldsymbol{X_C} = \left[\frac{\Delta \boldsymbol{H_m} - \Delta \boldsymbol{H_{cc}}}{\Delta \boldsymbol{H_m^0} \bullet (1 - \boldsymbol{w})} \mathbf{x} 100\right] \quad (1)$$

Where ΔH_m is the thermodynamic melting enthalpy (Jg^{-1}) of each sample taken from the thermal-curves of the reheat cycle, ΔH_{cc} is the cold crystallization enthalpy (Jg^{-1}), ΔH^0_m is considered as the theoretical melting enthalpy of a 100% crystalline PLA, i.e., 93.0 (Jg^{-1}) [47] and (1- w) corresponds to the weight fraction of PLA in the samples.

The thermomechanical characterization, of neat PLA and its blends with gum rosin esters, was carried on an oscillating rheometer AR G2 from TA Instruments (New Castle, USA). The tests were done over testing specimens sizing 40 × 10 × 4 mm^3, with a temperature program from 30 to 130 °C, at a heating ramp of 2 °C min^{-1}, maximum deformation (γ) of 0.1%, and a frequency of 1 Hz.

In addition, Vicat softening temperatures (VST) and Heat deflection temperature (HDT) were assessed in a Vicat/HDT compact equipment Deflex 687-A2 from Metrotec S. A (Sebastian, Spain), in a heating bath with silicone oil. VST values were obtained using method B50 of ISO 306, with a standard flat-ended-needle. HDT measurements were obtained according to method A of ISO 75. Both tests were performed with rectangular injected-molded specimens sizing 80 × 10 × 4 mm^3.

Tensile Properties

The tensile properties of PLA-gum rosin ester blends were obtained according to ISO 527-2 guidelines [44], conducted on standards testing samples (dumbbell-shape "1BA" type) as referred on the standard. Tests were done in a universal tensile tester machine ELIB 30 from S.A.E. Ibertest (Madrid, Spain) using a loading speed of 10 mm min^{-1}, with a load cell of 5 kN. Five samples were tested for each formulation and the average values of the calculated tensile strength (MPa), tensile modulus (MPa) and elongation at break (%) were reported. In addition, Charpy impact test was carried out to determine the energy absorption of the materials, by using a 6 J Charpy pendulum in an impact test machine from Metrotec, S. A, (San Sebastián, Spain), under ISO 179 standard. Five specimens without notch were tested for each formulation, at room conditions (24 °C and relative humidity of 35%).

Field Emission Scanning Microscope (FESEM)

The microstructure assessments of PLA-gum rosin blends were conducted in a field emission scanning microscope

(FESEM) ZEISS Ultra-55 from Oxford-Instruments (Oxfordshire, United Kingdom) operated at 2 kV. The images recording was done on broken specimen surfaces of the impact tests, mounted in a sample holder using conductive carbon adhesive tape, and coated with a thin layer of gold-palladium alloy for better conductivity, employing a Emitech SC7620 Sputter-Coater from Quorum Technologies (East Sussex, UK).

Results and Discussion

FTIR Measurements

The FTIR spectra of UTP and UTG are shown in Fig. 2, as well as the FTIR spectra of PLA and PLA-gum rosin ester blends. The results of (FTIR) spectral analysis allowed us to validate both commercial rosin derivatives as gum rosin esters. The peak exhibited at 1726 cm^{-1} for UTP and UTG gum rosin esters in (Fig. 2a and b) correspond to the stretching vibration of (C = O ester), which occurs after the esterification reaction [38, 48] derived from rosin acids and the –OH hydroxyl groups of pentaerythritol (four hydroxyl groups) and glycerol (three hydroxyl groups), in good accordance with that formerly reported by Aldas et al. (2020), who observed that in a pentaerythritol rosin ester the characteristic groups are found at the 1727 cm^{-1}, representative of the -C = O stretching of the ester group [49]. For neat PLA spectrum, the typical stretching of carbonyl group (C = O) of lactide is located at 1757 cm^{-1} as a high intensity peak [50]. The asymmetric and symmetric stretching of the methyl group (CH_3) is observed as a band with double peak at 2992 and 2957 cm^{-1}. The asymmetric and symmetric bending of the methyl group (CH_3) bands are located at 1455 and 1365 cm^{-1}, respectively. Finally, the -C-O bond stretching vibration is found as low intensity peaks at 1040 and1256 cm^{-1} [51, 52]. When analyzing the FTIR spectra of PLA-gum rosin ester blends (Fig. 2a and b), no significant differences were observed when compared to the spectrum of neat PLA, other than the small absorption peaks located between 1800 – 1500 cm^{-1}, according to the literature, corresponding to typal peaks of gum rosin esters, gathering much attention the peak located at 1460 cm^{-1} ascribed to the scissoring vibration of -CH2- in gum rosin esters [38, 53, 54]. In addition, an increasing intensity of the stretching vibration of the carbonyl group (C = O) of PLA was observed. This could be attributed to a successful incorporation of gum rosin esters into PLA matrix, since the rosin's characteristic groups are found in the same range of the stretching vibration of the carbonyl group of PLA. Therefore, the increasing intensity of the peak at 1757 cm^{-1} with the increasing content of gum rosin esters in the blends is assumed to be associated to the interfacial adhesion of the gum rosin esters with the PLA matrix, that in return causes higher energy absorption before rupture from the impact test in the formulations with lower content of gun rosin ester. This result can be correlated with the observed microstructure in the blends, where spherical domains were formed without surrounding empty space between the PLA matrix and the domains of the gum rosin esters.

Melt Flow Index and Processability Evaluation

Initially, MFI of neat PLA was investigated, and it was found to be 17 g/10 min (a higher value than the MFI value indicated in the technical data sheet of the supplier, 3 g/10 min). It should bear in mind that, technical data sheets give typical properties values, which are suggested not to be construed as specifications. Subsequently, the MFI of PLA-gum rosin ester blends was investigated at the same test condition of low shear rate under constant load. The results of MFI measurements, shown in Fi g. 3, indicate that the addition of gum rosin esters increases the MFI of PLA with the increasing content of gum rosin esters, facilitating the movement of the polymer chain in the molten state. It should be highlighted that both gum rosin esters are compounds with low softening points between 86 and 115 °C. Therefore, the increment of MFI values could be ascribed

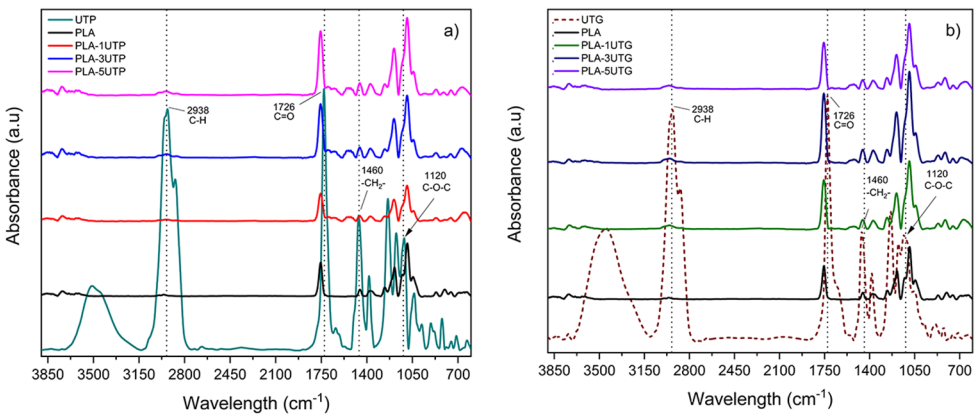

Fig. 2 FTIR spectra of (**a**) UTP gum rosin ester and PLA/UTP, (**b**) UTG gum rosin ester and PLA/UTG.

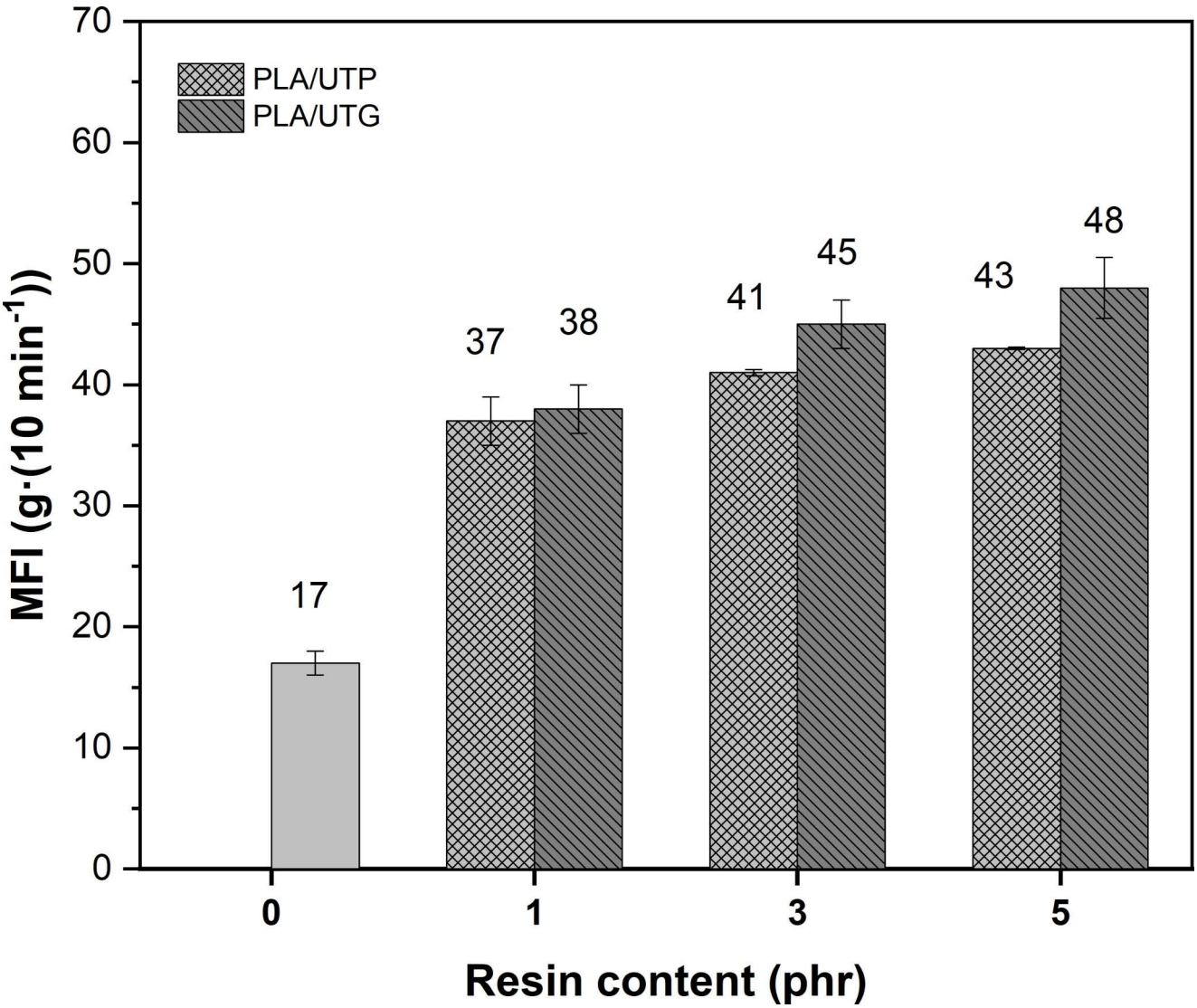

Fig. 3 MFI comparative trends of neat PLA and its blends with gum rosin esters

to a lubricating action [43] provided by the gum rosin esters incorporation, reducing the internal friction in polymer-polymer interaction and allowing the material to easily flow [55]. The lubricating action could be also promoted due to the low molecular weights of the gum rosin esters (UTG 945–1100 g/mol and UTP 2074 g/mol), thus the molecular structure of gum rosin esters provides greater movement of the PLA polymer chain in the molten state. In addition, the fact that the additives themselves contain ester groups makes them chemically compatible since PLA also contains ester groups. Therefore, this facilitates the good interaction between both, promoting the additives to homogenize in the PLA matrix allowing a lower friction between the PLA chains.

Moreover, it was observed that UTG addition causes a slightly higher increment in MFI values than UTP. This could be explained given that UTG is a glycerol gum rosin ester with lower molecular weight and lower softening point (as shown later in DSC analysis) compared with UTP-pentaerythritol gum rosin ester. Therefore, those factors also influence the tackifier and viscosity behavior of the gum rosin esters. Furthermore, after the incorporation of gum rosin esters, a notable change in the injection molding parameters was observed (see Table 2). Neat PLA testing samples were injected at an average temperature of 180 °C,

meanwhile, PLA-gum rosin esters blends were injected at an average temperature of 20 °C lower. This behavior, in correlation with the increment of MFI values, indicates that 160 °C can be considered as a suitable temperature to achieve the adequate fluidity in the injection molding process. In addition, the required injection pressure for PLA samples (110 Bar) decreased of more than 30% during the PLA-gum rosin esters blends injection (70 Bar), consequently, the packing pressure was also decreased of about 38%. An additional improvement aspect can be seen in the increased capacity of the mold filling, going from incorporating 35 cm^3 to incorporating 45 cm^3. As the MFI of the formulations with gum rosin esters increases, the melt completely fills the mold cavity. From the technical point of view, the use of gum rosin esters as lubricant additives on polylactide polymer could be of high interest for industrial applications, due to the fact that it is a material based on a renewable resource, able to provide excellent lubricating properties in the molten polymer, reducing, in turn, the equipment wear and energy consumption [56].

Thermal Evaluation and Thermomechanical Properties Measurements

Thermal Stability

To evaluate the effect of gum rosin esters (UTP and UTG) over the thermal stability of PLA, thermogravimetric analysis was performed. TGA thermal parameters obtained from the dynamic heating cycle have been summarized in Table 3. Weight loss and derivative curves (DTG) of gum rosin esters and PLA blends are reported in Figs. 4 and 5, respectively.

Initial characterization of the gum rosin esters was performed. It was found that both gum rosin esters degrade in a two steps process, initiated by hydrogen absorption followed by a second-order reaction and activation energy as described in the literature [57, 58]. Also, it is known that unmodified gum rosin´s thermal and oxidation stability is governed solely by the resin acids, which present a high susceptibility to react in the presence of oxygen, due to the conjugated double bonds in levopimaric and abietic acids. However, in the nitrogen atmosphere, gum rosin remains stable when heated up to 200 °C. In the case of gum rosin esters, it exhibits greater thermal stability, over 300 °C [38]. As previously reported by M. Aldas et al. [29], the onset thermal decomposition ($T_{5\%}$) of UTP was located around 316 °C, with a maximum degradation peak (T_{max}) at 445 °C and a second thermal degradation step at 570 °C. Whereas, lower $T_{5\%}$ located around 310 °C was found for UTG, with a T_{max} at 416 °C and a second thermal degradation step at 550 °C. Despite the small difference of about 6 °C on $T_{5\%}$, between the two gum rosin esters, results corroborate the information found on literature regarding the higher thermal stability of pentaerythritol rosin ester (due to its chemical structure) over glycerol rosin ester [48, 59].

On the other hand, the evaluation of TGA curves from Fig. 4a reveals that the presence of gum rosin esters into PLA matrix did not produce remarkable increase on the thermal stability of PLA, since PLA-gum rosin ester blends showed similar decomposition pattern (a single step process) as in the case of neat PLA. However, meanwhile neat PLA exhibited a $T_{5\%}$ at 341 °C with a maximum decomposition rate at 370 °C, PLA-gum rosin ester blends presented a $T_{5\%}$ in the range of 342–344 °C, with a difference of about 3 °C. These results suggests that gum rosin esters incorporation on PLA improves slightly the thermal stability of lactic

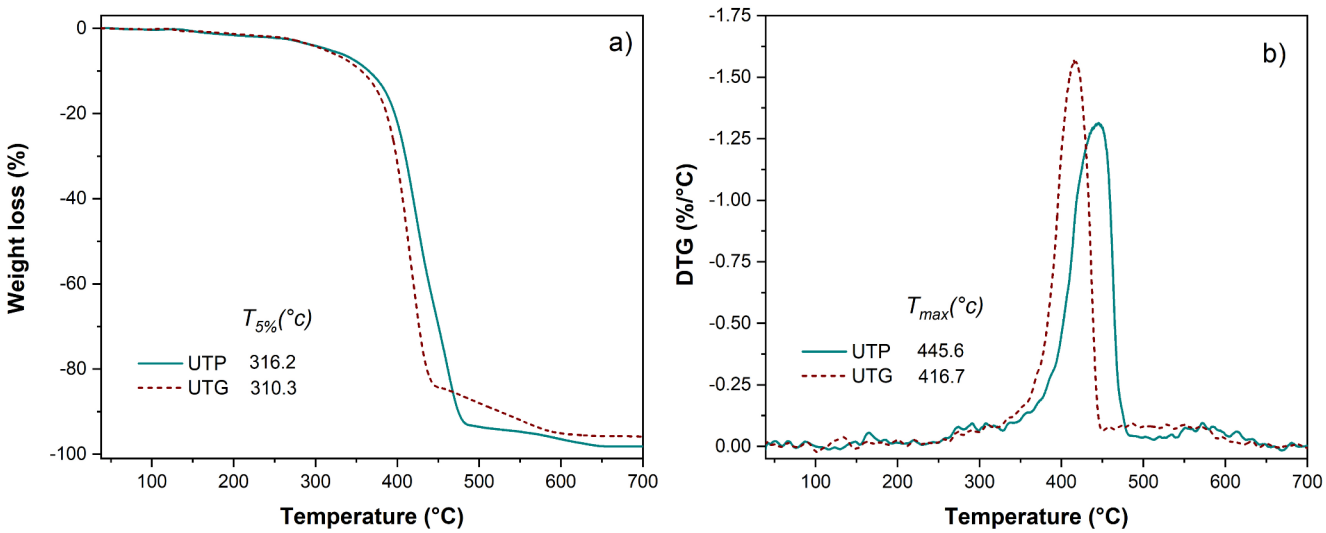

Fig. 4 Plot evaluation of TG (**a**) and DTG (**b**) curves of the gum rosin esters

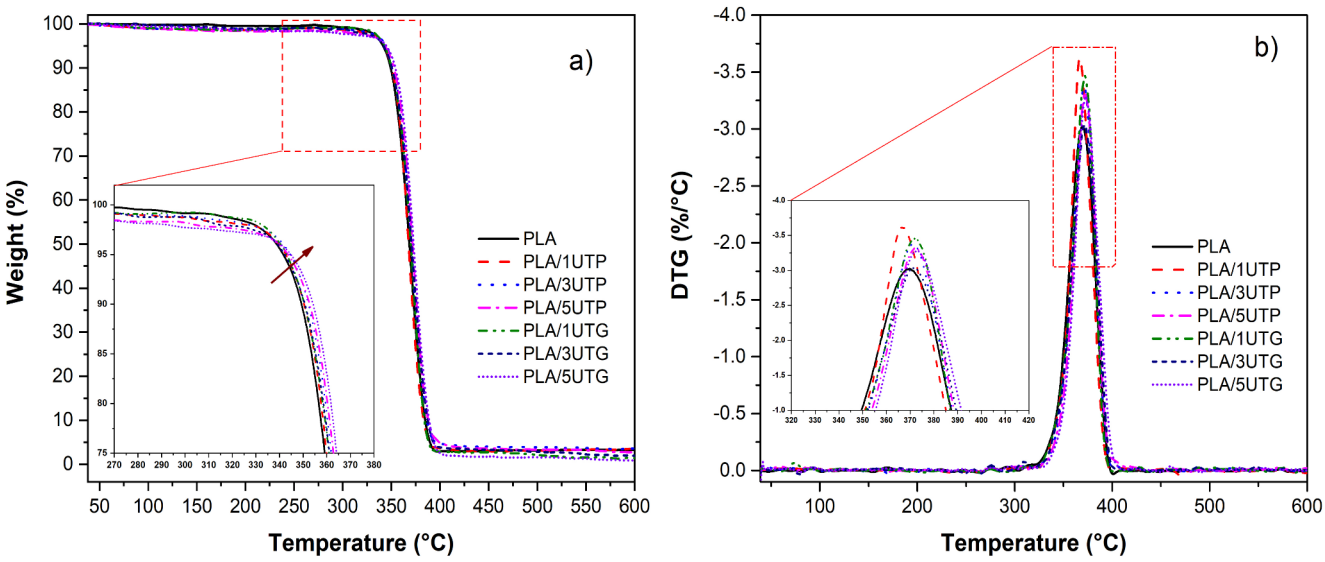

Fig. 5 Plot evaluation of TG (**a**) and DTG (**b**) curves of neat PLA and its blends with gum rosin esters (UTP and UTG).

Table 3 DSC thermal properties and TGA principal parameters of neat PLA and its blends with gum rosin esters (UTP and UTG).

Samples	*DSC (at a heating rate of 10 °C min^{-1})*					*TGA*		
	T_g(°C)	T_{cc}(°C)	$\Delta H_{cc}(Jg^{-1})$	T_m(°C)	$\Delta H_m(Jg^{-1})$	X_c(%)	$T_{5\%}$(°C)	T_{max}(°C)
PLA	61.8	131.5	20.7	159.3	22.1	1.5	341.7	370.2
PLA/1UTP	61.2	138.9	3.6	158.8	4.9	1.4	342.0	368.5
PLA/3UTP	61.0	142.1	0.7	158.8	2.2	1.7	343.6	370.6
PLA/5UTP	61.0	142.2	0.6	158.2	2.2	1.7	344.6	371.5
PLA/1UTG	61.6	138.9	1.5	158.1	1.8	0.3	342.0	372.0
PLA/3UTG	61.4	138.7	1.5	158.0	1.7	0.3	342.4	373.0
PLA/5UTG	61.3	132.4	3.2	158.0	3.3	0.1	342.9	372.0

acid polymer, considering the grade of PLA used to run the experiment.

Moreover, a reduction of thermal stability of PLA-gum rosin ester blends could have been expected, due to the lower $T_{5\%}$ of gum rosin esters, about 25 °C lower than $T_{5\%}$ value for PLA. Nevertheless, the amount of gum rosin esters used on the formulations is presumed to be well mixed and dispersed into polymer matrix, which does not allow the gum rosin esters molecules to degrade within their typical temperature range (310–316 °C). This behavior was also observed on the maximum degradation rate, where temperatures kept within the range of 368–373 °C, associated with the limited effect produced by the quantities of gum rosin esters incorporated (1–5 phr). It is worth to mention the disagreeing effect observed by C. Pavon et al. [35], who used pentaerythritol rosin ester to modify polybutylene adipate terephthalate (PBAT), describing the successful enhancement of PBAT thermal stability by increasing its $T_{5\%}$ in at least 10 °C by adding only 5 phr of gum rosin ester. To this effect, it can be state that depending on the chemistry of the polymer matrix, the pentaerythritol rosin ester will have a positive or negative effect.

Differential Scanning Calorimetry

The effect of gum rosin esters on the main thermal transitions of PLA matrix was investigated by using differential scanning calorimetry (DSC). Prior DSC analysis of the gum rosin esters was carried out, and their DSC thermograms depicted in Fig. 6a show a drop on the baseline at 53.3 °C for UTG, whereas UTP presents a baseline drop at 62.6 °C, confirming the higher susceptibility of UTG against temperature compared with UTP, in good accordance with the TGA results previously reported. DSC thermograms of neat PLA and PLA-gum rosin ester blends, taken from the second heating ramp, are plotted in Fig. 6b, c. Besides, the detailed thermal parameters are summarized in Table 3. As it can be observed, neat PLA showed a characteristic glass transition temperature (T_g) close to 62 °C, clearly identified by the change of the slope in the heat flow curve in Fig. 6b. The exothermic peak located around 131 °C associated with the cold crystallization process and the endothermic peak at 159 °C, related to the melting temperature (T_m) were also identified. These results are typical of amorphous

polylactide polymer, similar to those previously reported by other studies [50, 60, 61].

After the incorporation of the gum rosin esters, no significant changes were observed in the T_g and T_m of PLA formulations. However, and despite that the polymer matrix used for running the experiment is a low flow and amorphous PLA, lower values of crystallization enthalpy (ΔH_{cc}) and melting enthalpy (ΔH_m) were identified in all formulations compared with the corresponding values obtained for neat PLA ($\Delta H_{cc} = 20.7$ Jg^{-1}; $\Delta H_m = 22.1$ Jg^{-1}), reaching values down to $\Delta H_{cc} = 0.6$ Jg^{-1} for PLA/5UTP and $\Delta H_m = 0.6$ Jg^{-1} for PLA/3UTG. The results suggest that the presence of gum rosin esters into amorphous PLA does not lead to new crystal growth, instead it prevents the crystal formation by slowing down the crystallization rate, thus reducing the values of ΔH_{cc} and ΔH_m during the heating ramp of 10 °C min^{-1}. Additionally, it can be supposed that the decrement of crystallization rate produces a delayed-on crystal formation, therefore, the slight increment of the cold crystallization temperature in all formulations, reaching values up to 142.2 °C for PLA/5UTP.

As it can be seen in Fig. 6b and c, the reduction of the cold crystallization peaks and melting peaks after incorporation of gum rosin esters did not significantly influenced the degree of crystallinity, being the values still representative of amorphous polylactide polymer. Disagreeing with this study, Mysiukiewicz et al. [62] observed a decreasing tendency of the cold crystallization peaks without reduction on the melting peaks, when studying the crystallization of polylactide-based green composites. They ascribed this phenomenon to changes in the nucleation of crystallites, where higher number of active nucleation centers are

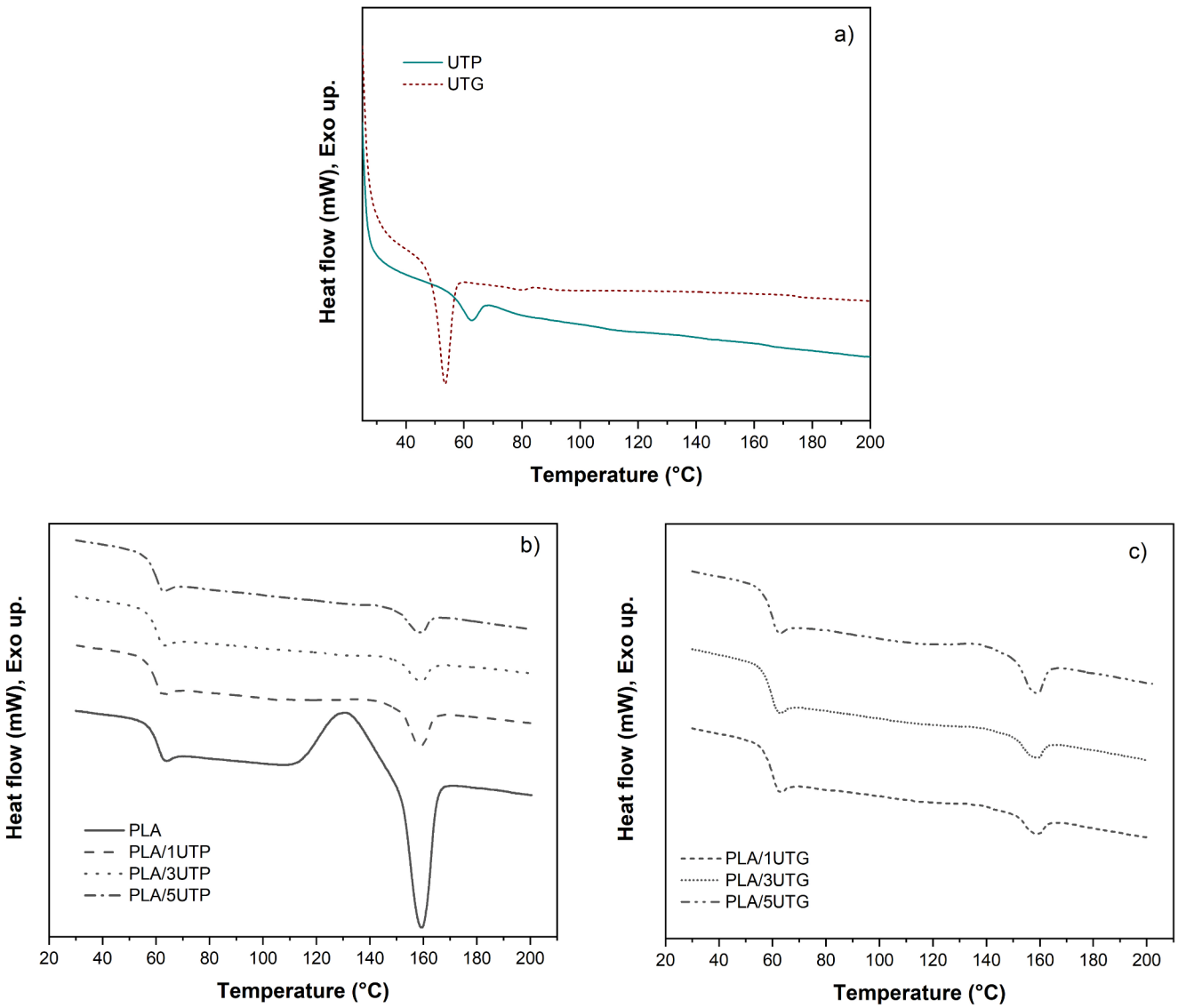

Fig. 6 Comparative plot of DSC curves of neat PLA and its blends with gum rosin esters, taken from the second heating cycle

formed during cooling rather than during the heating cycle. It is worthy to mention that, in this study, no evidence of melt crystallization process was observed during the cooling ramp.

Dynamic mechanical thermal analysis (DMTA).

To better understand the effect of gum rosin esters on PLA stiffness and the visco-elastic response of PLA-gum rosin ester blends, a dynamic mechanical-thermal analysis of produced blends has been carried out and compared with neat PLA. Figure 7a, b shows the variation of the storage moduli (*G'*) (representing the elastic properties) and the damping factor (tan *δ*) (representing the ability of elastic strain energy dissipation) both as a function of temperature.

As it is well-known, PLA presents high *G'* value in the glassy state at room temperature due to its intrinsic stiffness. In Fig. 7a, a notable reduction of *G'* values can be observed from 30 to 90°C in presence of the additives. This reduction of *G'* values for PLA-gum rosin esters blends could be associated with a positive effect of gum rosin esters presence, which induce a decrement of the material stiffness. It is assumed that this behavior, in turn, facilitates the material's processability by making it less challenging to be forced through the screw and nozzle of an extruder [63].

Additionally, the sudden decline of *G'* values between 60 and 70 °C, ascribed to polymer chains relaxation during the glass transition interval, also shows the limited capacity of gum rosin esters to plasticize PLA, since the curves were not significantly shifted to lower temperature (indicating no high reduction of T_g) in correlation with the DSC analysis. Further, in Fig. 7b it can be observed the slight increment of tan δ after gum rosin esters incorporation into PLA. Tan δ is yet another approach to identify the T_g by locating the maximum peak [64], but also Ferri et al [65], ascribed the height of tan δ to the motion of amorphous phase in the polymer matrix. Thus, it is assumed that the slight increment of tan *δ* is associated with an improved ability of PLA-gum rosin esters blends to dissipate elastic strain energy during deformation, compared to neat PLA.

The determination of Vicat softening temperature (VST) and the heat deflection-temperature (HDT) were complementary to corroborate the effect of gum rosin esters on the thermal behavior of PLA. Specifically, HDT was useful to correlate the results obtained by DSC analysis. According to literature [66, 67], one method to improve the heat resistance of PLA is by increasing its crystallinity. Y. Liu et al. [68], reported the improvement of PLA crystallinity by the addition of a nucleating agent. Consequently, PLA exhibited an enhanced heat resistance, evidenced by a considerable increment of the heat deflection temperature. In this study, as reported in the DSC analysis section, the crystallinity degree of PLA was poorly affected by the incorporation of gum rosin esters, therefore, no noticeable changes of HDT values were expected. As it can be seen in Table 4, HDT values of all formulations remained without noticeable variation compared with neat PLA.

Moreover, the VST values, also reported in Table 4, shows a negligible variation of 1 °C, which indicates no crystallinity enhancement, thus, no improvement of heat resistance of PLA was observed after the incorporation of gum rosin esters. This is closely associated with the loss of storage modulus shown in the DMTA results, given the fact that loading stress cannot be endured by disarranged and tangled amorphous phase.

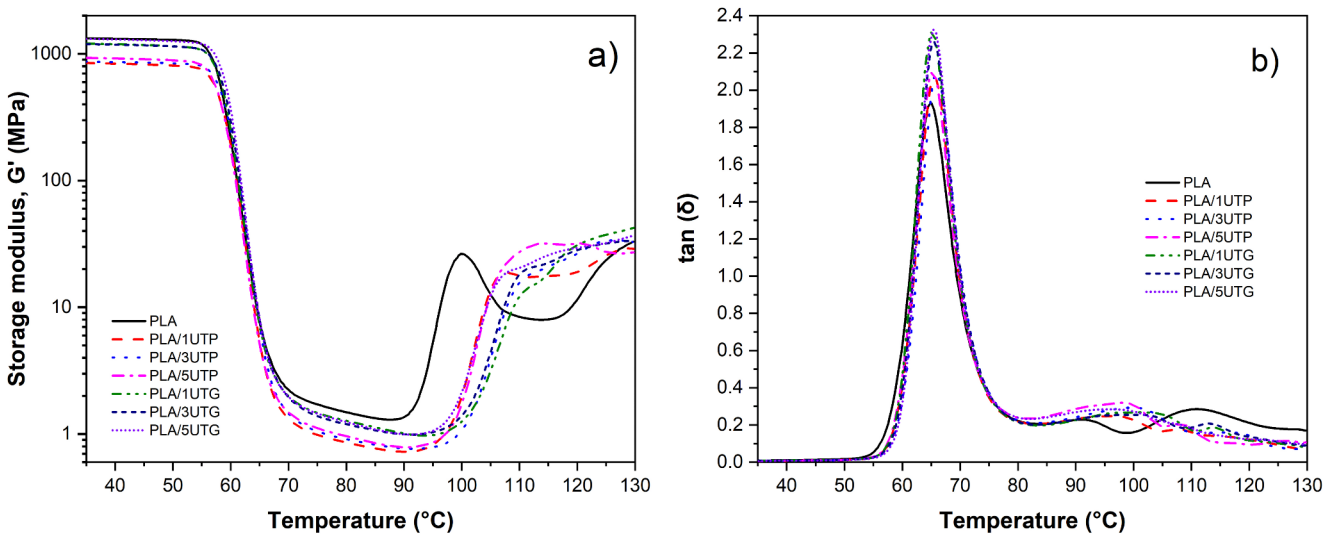

Fig. 7 Comparative storage modulus (*G'*) (**a**) and damping factor (*tan δ*) (**b**) curves for of neat PLA and its blends with gum rosin esters (UTP and UTG).

Table 4 Measurements of Vicat softening temperature and heat deflection temperature of neat PLA and its blends with gum rosin esters (UTP and UTG).

Samples	Vicat softening temperature, VST (°C)	Heat deflection temperature, HDT (°C)
PLA	57.1 ± 0.4	54.7 ± 0.5
PLA/1UTP	56.3 ± 0.3	54.4 ± 0.6
PLA/3UTP	56.1 ± 0.5	54.3 ± 0.4
PLA/5UTP	56.0 ± 0.4	54.3 ± 0.3
PLA/1UTG	56.1 ± 0.3	54.5 ± 0.5
PLA/3UTG	56.0 ± 0.5	54.2 ± 0.4
PLA/5UTG	55.9 ± 0.3	54.0 ± 0.5

Mechanical Properties

In addition to thermomechanical characterization, the PLA-gum rosin ester blends were evaluated in terms of their response when tensile and impact forces are applied. Figure 8 depicts the mechanical properties evolution of PLA injected-molded parts as a function of the gum rosin esters varying content. As it can be observed, in Fig. 8a PLA tensile strength values remained without relatively appreciable changes. However, a remarkable decreasing trend in tensile modulus occurred with the increasing gum rosin esters content, see Fig. 8b. This reduction of tensile modulus was even more pronounced in the case of UTG addition compared with UTP, especially from contents greater than 3 phr. Tensile modulus decreased from 3142 MPa (neat PLA) down to 2194 MPa and 1565 MPa with 5 phr content of UTP and UTG, respectively.

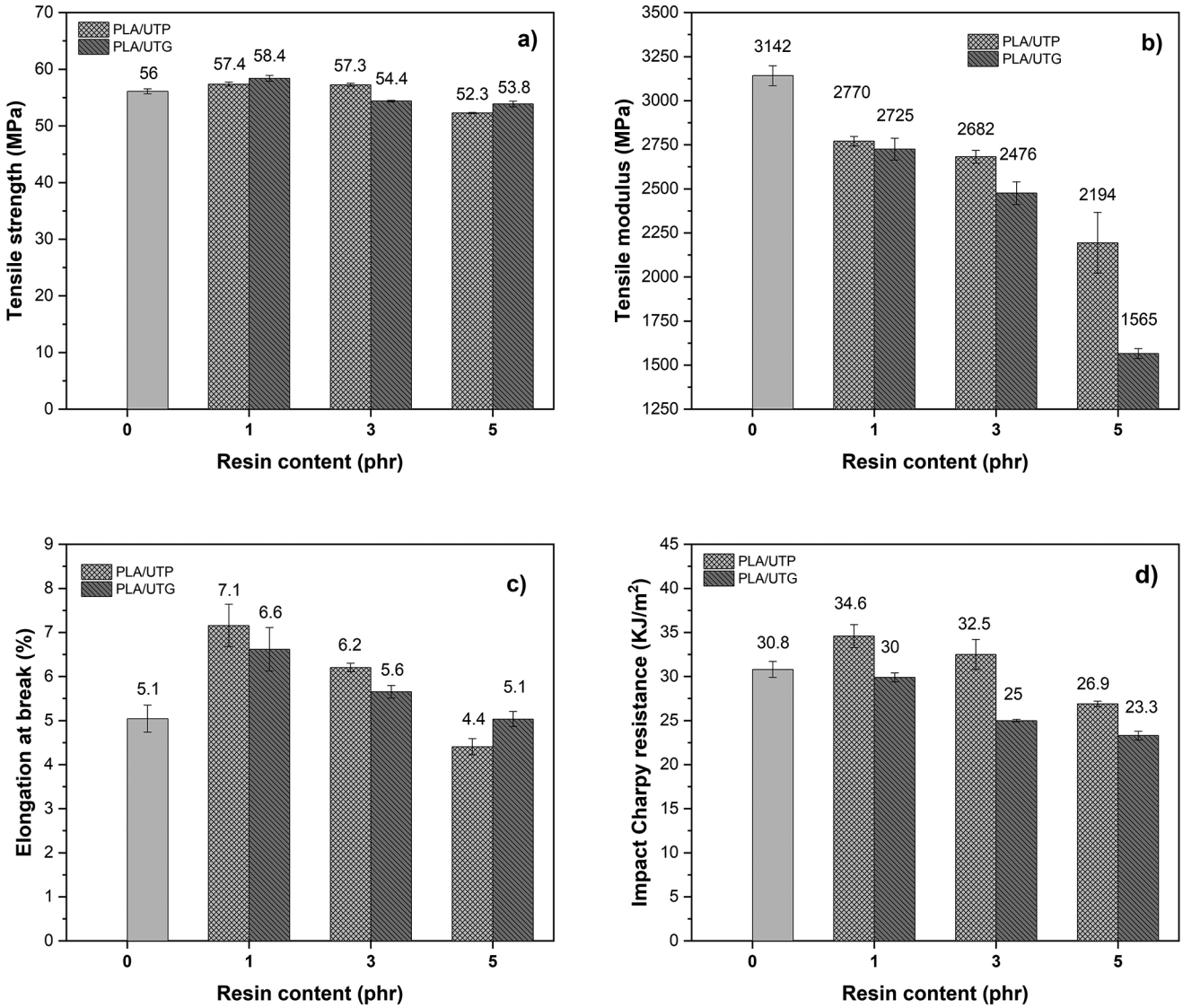

Fig. 8 Plot evaluation of gum rosin esters effect on the mechanical properties of PLA formulations. Tensile strength (**a**), Tensile modulus (**b**) and Elongation at break (**c**) and Impact Charpy resistance (**d**)

It is well known that a plasticization process leads to change the mechanical response of a given polymer by lowering the tensile strength and modulus, along with the increment of the ductility [69–72]. Interestingly, the results reported herein show the typical reduction of tensile modulus, nevertheless, the tensile strength values remain with a slight variation in a narrow range of 4 MPa. This behavior could be explained due to a possible scarcely plasticizing action of gum rosin esters, and partial miscibility with PLA matrix, which allow the material to undergo higher deformation before rupture. This effect can be evidenced by the slight increment of elongation at break showed by the formulations with 1 and 3 phr content of UTP and UTG (Fig. 8c), along with the increment of the impact energy absorption showed in Fig. 8d. Furthermore, the abrupt decrement of tensile modulus, elongation at break and impact energy absorption showed by the formulations with 5 phr content of UTP and UTG, is attributed to a saturation effect of the gum rosin esters into PLA. UTG and UTP saturations act as stress concentrators that, under impact conditions, do not allow the material to absorb the higher amount of energy as it should. On the other hand, although at high UTG and UTP contents there are signs of higher ductility, partly due to the effect of plasticization, and a lower Young's modulus associated with this effect, the saturations prevent the material from having a high elongation at break.

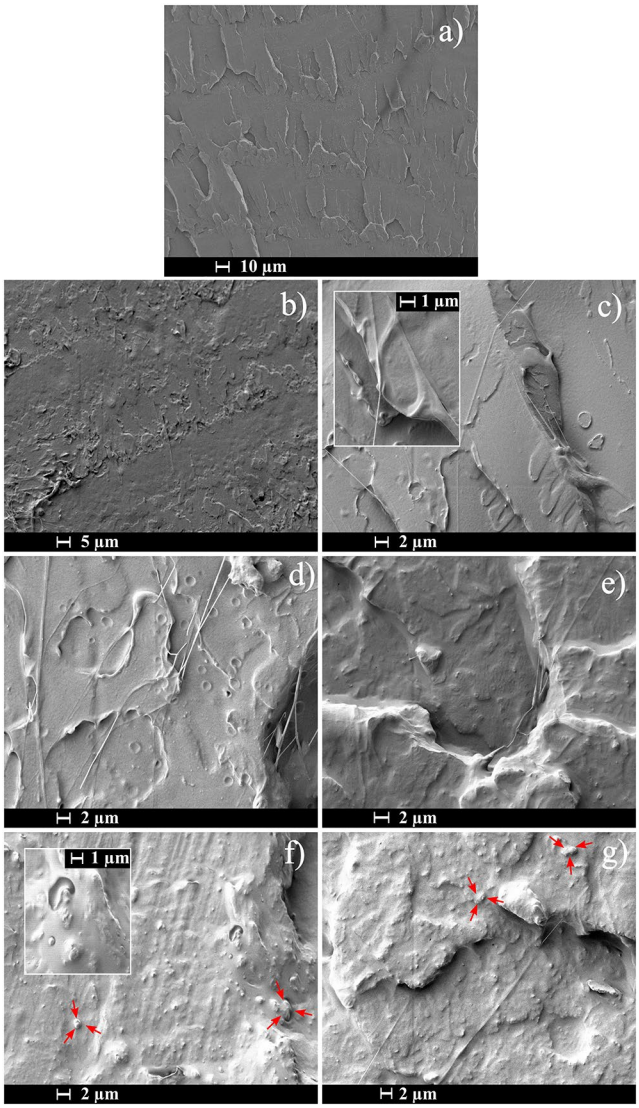

Fig. 9 Fractured surfaces images from impact test samples of PLA, PLA/UTP and PLA/UTG blends, observed by FESEM: (**a**) PLA at 2000x, (**b**) PLA/1UTP at 2000x, (**c**) PLA/1UTG at 2000x, (**d**) PLA/3UTP at 2000x, (**e**) PLA/3UTG at 2000x, (**f**) PLA/5UTP at 2000x and (g) PLA/5UTG at 2000x

Microstructural Evaluation

The microstructural assessment was performed to reach a deep understanding of gum rosin esters interaction with PLA matrix and correlate the physical properties of the polymeric systems. The microstructure images of neat PLA and PLA-gum rosin ester blends are shown in Fig. 9. As it can be observed in Fig. 9a, the micrograph reveals the typical brittle fracture of neat PLA with smooth surface and sharp cracks due to its inherent fragility [28, 73]. These sharp cracks indicate that once fissures initiation occurred, they suddenly expanded causing an abrupt rupture of the material. However, along with the increasing content of gum rosin esters, roughness starts to appear on the fractured micro-surface of the polymer systems. From one side, formulations with 1 phr content of gum rosin esters (Fig. 9b, c) shows small threads, which indicate tearing of materials during the rupture. As content of gum rosin esters increases in the blends (Fig. 9d, e, formulations with 3phr), the number of threads and roughness is more noticeable. This suggests that the material has suffered a higher level of tearing during the rupture and, consequently, higher deformation. In addition, the filaments formed are due to increased ductility due to plasticization, which indicates that UTP and UTG are compatible with the PLA matrix. These filaments are more present in the formulations that contains UTP.

On the other hand, formulations with 5 phr content of gum rosin esters showed completely difference morphology, as shown in Fig. 9f and g. In this case, it is possible to observe the scarce dispersion of the gum rosin esters particles within the PLA matrix, becoming less uniform as the gum rosin esters content increases. This, as evidenced by the formation of little lumps with irregular shapes (emphasized with red arrows), leads to a clear immiscibility by phase separation. The formation of the little lumps is associated to a saturation of the gum rosin esters in PLA matrix, which are agglomerated into small microdomains. Thus, it is assumed that the maximum quantity of gum rosin esters efficient for PLA performance improvement is close to 3 phr. If we consider

that the saturations of UTP are lower than those of UTG, it can be concluded that this is due to a higher compatibility or chemical affinity between UTP and PLA than in the case of UTG. In turn, greater compatibility implies better dispersion and therefore, improved processability. In addition, it was observed that the microdomains, in red arrows, are not surrounded by empty space. This suggest that the microdomains are not separated from the polymer matrix, therefore, it is supposed that some interfacial adhesion between gum rosin esters and PLA matrix has occurred, as later confirmed by FTIR analysis. Nevertheless, in good accordance with the mechanical properties, it could be stated that UTP had better interaction with PLA compared to UTG. It is worth mentioning the separate case previously reported by Aldas et al. [49], who also observed better interaction of pentaerythritol ester of gun rosin in a mixture with thermoplastic starch, than when using another kind of gun rosin products.

Conclusions

PLA and gum rosin esters blends (pentaerythritol ester and glycerol ester) have been successfully prepared by melt extrusion. The resulting formulations showed a significant increase of the MFI values in at least 100% compared to neat PLA with the addition of only 1 phr content of gum rosin esters. Consequently, this positive behavior led to reduce the injection process temperature by at least 20 °C due to the improved fluidity of the prepared formulations. Besides that, the required injection pressure for neat PLA samples (110 Bar) dropped in more than 30% during the PLA-gum rosin esters blends injection (70 Bar), leading the packing pressure also decrease in about 38%. It is worthy to highlight that the improvement of these factors directly entails to the reduction of the equipment wear and energy consumption. Since gum rosin esters act as external lubricants, tensile strength values remained almost constant, followed by a slight increase in elongation at break and impact energy absorption for formulations with lower pentaerythritol ester content (1 and 3 phr). In addition to improving PLA processability (they can be processed 20 °C lower), these gum rosin esters slightly improve PLA thermal stability (around 3ºC higher). Finally, the morphological evaluation, correlated with the mechanical properties, showed that UTP had better interaction with PLA compared to UTG. As well, it revealed the good dispersion and incorporation of gum rosin esters into PLA in concentration lower than 5 phr. Meanwhile, concentrations equal to 5 phr presented formation of little lumps with no surrounding empty space. Therefore, UTP and UTG have been demonstrated as potential biobased external lubricating agents to improve PLA processability.

Acknowledgements H. de la Rosa thanks UPV for the grant received through the (FPI-2018-S2-31946) program and the UPV doctoral school for the interchange mobility grant (Resolution. 16/12/21). UPV authors thank United Resins—Produção de Resinas S.A. (Figueira da Foz, Portugal) for kindly supplying the gum rosin esters and for the collaboration in Project nº E! 114728 "Development and demonstration of innovative bio-resin-based polymers for industrial applications" - DDIBIORESIN (Project EUREKA – EUROSTARS 2).

Author Contributions Conceptualization HDR, MDS; Formal analysis, HDR, FD, JMF; Funding acquisition JLM, MDS; Investigation HRD, MDS, FD, JMF; Methodology HDR, DP, FD; Project administration JLM, MDS; Resources JLM, LT; Supervision MDS; Validation LT, DP, FL; Visualization HDR, FD; Roles/Writing - original draft HDR, FD, FL; Writing - review & editing HDR, DP, FD, MDS.

Funding This research was funded by MCIN/AEI/10.13039/501100011033 through PID-AEI Project (grant PID2021-123753NA-C33 and PID2020-116496RB-C22) and TED-AEI Project (grants TED2021-129920 A-C43), and, as appropriate, by "ERDF A way of making Europe", by the "European Union" or by the "European Union NextGenerationEU/PRTR".
Open Access funding provided thanks to the CRUE-CSIC agreement with Springer Nature.

Declarations

Competing Interests The authors declare no competing interests.

References

1. Pious CV, Thomas S (2016) Polymeric Materials—Structure, Properties, and Applications. Printing on Polymers: Fundamentals and Applications 21–39. https://doi.org/10.1016/B978-0-323-37468-2.00002-6
2. Wang G, He M, li, Jiang D et al (2017) The properties of neutron shielding and flame retardant of EVA polymer after modified by EB accelerator. Radiat Phys Chem 140:322–327. https://doi.org/10.1016/j.radphyschem.2017.03.038
3. Mural PKS, Rana MS, Madras G, Bose S (2014) PE/PEO blends compatibilized by PE brush immobilized on MWNTs: improved interfacial and structural properties. RSC Adv 4:16250–16259. https://doi.org/10.1039/c4ra01961j
4. Ronca S (2017) Polyethylene. Brydson's Plastics Materials: Eighth Edition. Butterworth-Heinemann, pp 247–278
5. Elmehbad NY, Mohamed NA (2021) Preparation and characterization of some new antimicrobial thermally stable PVC

formulations. Polym Bull 78:6183–6204. https://doi.org/10.1007/s00289-020-03433-8
6. Sterky K, Jacobsen H, Jakubowicz I et al (2010) Influence of processing technique on morphology and mechanical properties of PVC nanocomposites. Eur Polymer J 46:1203–1209. https://doi.org/10.1016/j.eurpolymj.2010.03.021
7. Fan R, Zhang W, Wang Y et al (2021) Metal material resistant to Hydrochloric Acid Corrosion. J Phys: Conf Ser 1732. https://doi.org/10.1088/1742-6596/1732/1/012134
8. Kumartasli S, Avinc O (2020) Important step in sustainability: polyethylene terephthalate recycling and the recent developments. Springer, Cham, pp 1–19
9. McAdam B, Fournet MB, McDonald P, Mojicevic M (2020) Production of polyhydroxybutyrate (PHB) and factors impacting its chemical and mechanical characteristics. Polymers 12:1–20
10. Briassoulis D, Tserotas P, Athanasoulia IG (2021) Alternative optimization routes for improving the performance of poly(3-hydroxybutyrate) (PHB) based plastics. J Clean Prod 318:128555
11. Jandas PJ, Mohanty S, Nayak SK (2013) Sustainability, compostability, and specific microbial activity on agricultural mulch films prepared from poly(lactic acid). Ind Eng Chem Res 52:17714–17724. https://doi.org/10.1021/ie4023429
12. Nooeaid P, Chuysinuan P, Pitakdantham W et al (2021) Eco-friendly polyvinyl Alcohol/Polylactic acid Core/Shell structured fibers as controlled-release fertilizers for sustainable agriculture. J Polym Environ 29:552–564. https://doi.org/10.1007/s10924-020-01902-9
13. Gan I, Chow WS (2018) Antimicrobial poly(lactic acid)/cellulose bionanocomposite for food packaging application: a review. Food Packaging and Shelf Life 17:150–161
14. Khosravi A, Fereidoon A, Khorasani MM et al (2020) Soft and hard sections from cellulose-reinforced poly(lactic acid)-based food packaging films: a critical review. Food Packaging and Shelf Life 23:100429
15. Alsaheb RAA, Aladdin A, Othman NZ et al (2015) Recent applications of polylactic acid in pharmaceutical and medical industries
16. Davachi SM, Kaffashi B (2015) Polylactic acid in Medicine. Polym Plast Technol Eng 54:944–967. https://doi.org/10.1080/03602559.2014.979507
17. Li G, Zhao M, Xu F et al (2020) Synthesis and Biological Application of Polylactic Acid. Molecules. (Basel, Switzerland) 25
18. Deb D, Jafferson JM (2021) Natural fibers reinforced FDM 3D printing filaments. In: Materials Today: Proceedings. Elsevier, pp 1308–1318
19. Li X, Ai X, Pan H et al (2018) The morphological, mechanical, rheological, and thermal properties of PLA/PBAT blown films with chain extender. Polym Adv Technol 29:1706–1717. https://doi.org/10.1002/pat.4274
20. Palai B, Mohanty S, Nayak SK (2020) Synergistic effect of polylactic acid(PLA) and poly(butylene succinate-co-adipate) (PBSA) based sustainable, reactive, super toughened eco-composite blown films for flexible packaging applications. Polym Test 83:106130. https://doi.org/10.1016/j.polymertesting.2019.106130
21. Chinsirikul W, Rojsatean J, Hararak B et al (2015) Flexible and tough poly(lactic acid) Films for Packaging Applications: property and processability improvement by effective reactive blending. Packaging Technology and Science. John Wiley and Sons Ltd, pp 741–759
22. Walha F, Lamnawar K, Maazouz A, Jaziri M (2018) Biosourced blends based on poly (lactic acid) and polyamide 11: structure-properties relationships and enhancement of film blowing processability. Adv Polym Technol 37:2061–2074. https://doi.org/10.1002/adv.21864
23. Marra A, Silvestre C, Duraccio D, Cimmino S (2016) Polylactic acid/zinc oxide biocomposite films for food packaging application. Int J Biol Macromol 88:254–262. https://doi.org/10.1016/j.ijbiomac.2016.03.039
24. Bajracharya GB, Koju R, Ojha S et al (2021) Plasticizers: synthesis of phthalate esters via FeCl3-catalyzed nucleophilic addition of alcohols to phthalic anhydride. Results in Chemistry 3:100190. https://doi.org/10.1016/j.rechem.2021.100190
25. Battegazzore D, Bocchini S, Alongi J, Frache A (2014) Plasticizers, antioxidants and reinforcement fillers from hazelnut skin and cocoa by-products: extraction and use in PLA and PP. Polym Degrad Stab 108:297–306. https://doi.org/10.1016/j.polymdegradstab.2014.03.003
26. Rajeshkumar G, Arvindh Seshadri S, Devnani GL et al (2021) Environment friendly, renewable and sustainable poly lactic acid (PLA) based natural fiber reinforced composites – A comprehensive review. J Clean Prod 310:127483
27. Scaffaro R, Lopresti F, Marino A, Nostro A (2018) Antimicrobial additives for poly(lactic acid) materials and their applications: current state and perspectives. Appl Microbiol Biotechnol 102:7739–7756
28. Ferri JM, Garcia-Garcia D, Montanes N et al (2017) The effect of maleinized linseed oil as biobased plasticizer in poly(lactic acid)-based formulations. Polym Int 66:882–891. https://doi.org/10.1002/pi.5329
29. Aldas M, Ferri JM, Lopez-Martinez J et al (2019) Effect of pine resin derivatives on the structural, thermal, and mechanical properties of Mater-Bi type bioplastic. J Appl Polym Sci 137:48236. https://doi.org/10.1002/app.48236
30. Quiles-Carrillo L, Duart S, Montanes N et al (2018) Enhancement of the mechanical and thermal properties of injection-molded polylactide parts by the addition of acrylated epoxidized soybean oil. Mater Des 140:54–63. https://doi.org/10.1016/j.matdes.2017.11.031
31. Quiles-Carrillo L, Blanes-Martínez MM, Montanes N et al (2018) Reactive toughening of injection-molded polylactide pieces using maleinized hemp seed oil. Eur Polymer J 98:402–410. https://doi.org/10.1016/j.eurpolymj.2017.11.039
32. de la Rosa-Ramirez H, Aldas M, Ferri JM et al (2020) Modification of poly (lactic acid) through the incorporation of gum rosin and gum rosin derivative: mechanical performance and hydrophobicity. J Appl Polym Sci 49346:1–15. https://doi.org/10.1002/app.49346
33. Qiu H, Chen X, Wei X et al (2020) The emulsifying properties of hydrogenated rosin xylitol ester as a biomass surfactant for food: Effect of pH and salts. Molecules 25:302. https://doi.org/10.3390/molecules25020302
34. Yadav BK, Gidwani B, Vyas A (2016) Rosin: recent advances and potential applications in novel drug delivery system. J Bioactive Compatible Polym 31:111–126. https://doi.org/10.1177/0883911515601867
35. Pavon C, Aldas M, de la Rosa-Ramírez H et al (2020) Improvement of pbat processability and mechanical performance by blending with pine resin derivatives for injection moulding rigid packaging with enhanced hydrophobicity. Polymers 12:1–19. https://doi.org/10.3390/polym12122891
36. Pathak YV, Nikore RL, Dorle AK (1985) Study of Rosin and Rosin esters as coating materials. Int J Pharm 24:351–354. https://doi.org/10.1016/0378-5173(85)90033-X
37. Rohani AB, Manroshan S, Devaraj V (2014) Evaluation of epoxidized natural rubber latex - based pressure sensitive adhesives containing hydrocarbon and rosin ester tackifier dispersions on adhesive properties. Advanced materials research. Trans Tech Publications Ltd, pp 189–193
38. Xu Z, Lou W, Zhao G et al (2019) Pentaerythritol rosin ester as an environmentally friendly multifunctional additive in vegetable oil-based lubricant. Tribol Int 135:213–218. https://doi.org/10.1016/J.TRIBOINT.2019.02.038

39. Mirabedini SM, Zareanshahraki F, Mannari V (2020) Enhancing thermoplastic road-marking paints performance using sustainable rosin ester. Prog Org Coat 139:105454. https://doi.org/10.1016/j.porgcoat.2019.105454
40. Aldas M, Pavon C, Ferri JM et al (2021) Films based on mater-bi® compatibilized with pine resin derivatives: Optical, barrier, and disintegration properties. Polymers 13:1506. https://doi.org/10.3390/polym13091506
41. Li Y, Liu X, Zhang Q et al (2018) Characteristics and kinetics of rosin pentaerythritol ester via oxidation process under ultraviolet irradiation. Molecules 23:2816. https://doi.org/10.3390/molecules23112816
42. H4R Consortium (2019) REACH registrations of Rosin, Rosin Salts and Rosin Esters. pp 1–54
43. Li Y, Niu M, Xu X et al (2020) Characteristics and kinetics of the glycerol ester of rosin: Via an oxidation process under ultraviolet irradiation. New J Chem 44:3375–3381. https://doi.org/10.1039/c9nj04439f
44. International Standards Organization (2012) ISO 527-2:2012. Plastics - determination of tensile properties - part, vol 2. Test conditions for moulding and extrusion plastics
45. International Standards Organization (2010) ISO 179-1:2010. Plastics - determination of Charpy impact properties - part, vol 1. Non-instrumented impact test
46. International Standards Organization (2012) ISO 1133-1:2012. Plastics - Determination of the melt mass-flow rate (MFR) and melt volume-flow rate (MVR) of thermoplastics - Part 1: Standard method
47. Huda MS, Drzal LT, Ray D et al (2008) Natural-fiber composites in the automotive sector. Properties and Performance of Natural-Fibre Composites. Elsevier Inc., pp 221–268
48. Xu Z, Lou W, Zhao G, et al (2019) Pentaerythritol rosin ester as an environmentally friendly multifunctional additive in vegetable oil-based lubricant. Tribology International 135:213–218. https://doi.org/10.1016/j.triboint.2019.02.038
49. Hardhianti MPW, Rochmadi, Azis MM (2022) Kinetic studies of esterification of rosin and pentaerythritol. Processes 10. https://doi.org/10.3390/pr10010039
50. Aldas M, Pavon C, López-Martínez J, Arrieta MP (2020) Pine resin derivatives as sustainable additives to improve the mechanical and thermal properties of injected moulded thermoplastic starch. Appl Sci (Switzerland) 10. https://doi.org/10.3390/app10072561
52. Venkatesh C, Laurenti M, Bandeira M et al (2020) Biodegradation and antimicrobial properties of zinc oxide–polymer composite materials for urinary stent applications. Coatings 10:1–22. https://doi.org/10.3390/coatings10101002
52. Yang S, Wu ZH, Yang W, Yang MB (2008) Thermal and mechanical properties of chemical crosslinked polylactide (PLA). Polym Test 27:957–963. https://doi.org/10.1016/j.polymertesting.2008.08.009
53. Chieng B, Ibrahim N, Yunus W, Hussein M (2013) Poly(lactic acid)/Poly(ethylene glycol) polymer nanocomposites: Effects of Graphene Nanoplatelets. Polymers 6:93–104. https://doi.org/10.3390/polym6010093
54. Zhang D, Zhou D, Wei X et al (2017) Green catalytic conversion of hydrogenated rosin to glycerol esters using subcritical CO2 in water and the associated kinetics. J Supercrit Fluids 125:12–21. https://doi.org/10.1016/j.supflu.2017.01.009
55. Karakus S, Ilgar M, Kahyaoglu IM, Kilislioglu A (2019) Influence of ultrasound irradiation on the intrinsic viscosity of guar gum–PEG/rosin glycerol ester nanoparticles. Int J Biol Macromol 141:1118–1127. https://doi.org/10.1016/j.ijbiomac.2019.08.254
56. Li Y, Niu M, Xu X, et al (2020) Characteristics and kinetics of the glycerol ester of rosin: Via an oxidation process under ultraviolet irradiation. New Journal of Chemistry 44:3375?3381. https://doi.org/10.1039/c9nj04439f
57. Meier-Haack J, Müller M, Lunkwitz K (2010) Polymers - Opportunities and Risks II: sustainability. Product Design and Processing
58. Höfer R (2012) Processing and Performance Additives for Plastics. Polymer Science: a comprehensive reference, 10 volume set. Elsevier, pp 369–381
59. Li Y, Xu X, Niu M et al (2019) Thermal Stability of Abietic Acid and its Oxidation Products. Energy Fuels 33:11200–11209. https://doi.org/10.1021/acs.energyfuels.9b02855
60. Liu P, Liu X, Saburi T et al (2020) Thermal Stability evaluation of Resin acids and Rosin Modified Resins. ACS Omega 5:29102–29109. https://doi.org/10.1021/acsomega.0c03736
61. Ladero M, de Gracia M, Trujillo F, Garcia-Ochoa F (2012) Phenomenological kinetic modelling of the esterification of rosin and polyols. Chem Eng J 197:387–397. https://doi.org/10.1016/J.CEJ.2012.05.053
62. Höhne CC, Schmidt R, Berner V et al (2021) Intrinsic flame retardancy of poly(lactic acid) bead foams. J Appl Polym Sci 138:50856. https://doi.org/10.1002/app.50856
63. Zhu YQ, Yang K, Edmonds L et al (2017) Silicone-covered biodegradable magnesium-stent insertion in the esophagus: a comparison with plastic stents. Therapeutic Adv Gastroenterol 10:11–19. https://doi.org/10.1177/1756283X16671670
64. Mysiukiewicz O, Barczewski M (2020) Crystallization of polylactide-based green composites filled with oil-rich waste fillers. J Polym Res 27:1–17. https://doi.org/10.1007/s10965-020-02337-5
65. Kimbell G, Azad MA (2021) 3D printing: Bioinspired materials for drug delivery. Bioinspired and Biomimetic materials for drug delivery. Elsevier, pp 295–318
66. Materials L (2019) Structure, characterization, and performance. Evaluation of Lignin-Modified Materials
67. Ferri JM, Motoc DL, Bou SF, Balart R (2019) Thermal expansivity and degradation properties of PLA/HA and PLA/βTCP in vitro conditioned composites. J Therm Anal Calorim 138:2691–2702. https://doi.org/10.1007/s10973-019-08799-0
68. Tábi T, Ageyeva T, Kovács JG (2021) Improving the ductility and heat deflection temperature of injection molded Poly(lactic acid) products: a comprehensive review. Polym Test 101:107282
69. Ma B, Wang X, He Y et al (2021) Effect of poly(lactic acid) crystallization on its mechanical and heat resistance performances. Polymer 212:123280. https://doi.org/10.1016/j.polymer.2020.123280
70. Liu Y, Jiang S, Yan W et al (2020) Crystallization morphology regulation on enhancing heat resistance of polylactic acid. Polymers 12:1–11. https://doi.org/10.3390/polym12071563
71. Ferri JM, Samper MD, García-Sanoguera D et al (2016) Plasticizing effect of biobased epoxidized fatty acid esters on mechanical and thermal properties of poly(lactic acid). J Mater Sci 51:5356–5366. https://doi.org/10.1007/s10853-016-9838-2
72. Torre L, Dominici F, Sanchez-Nacher L et al (2018) Manufacturing and compatibilization of PLA/PBAT binary blends by cottonseed oil-based derivatives. Express Polym Lett 12:808–823. https://doi.org/10.3144/expresspolymlett.2018.69
73. Ferri JM, Garcia-Garcia D, Rayón E et al (2020) Compatibilization and characterization of polylactide and biopolyethylene binary blends by non-reactive and reactive compatibilization approaches. Polymers 12:1344–1364. https://doi.org/10.3390/POLYM12061344
74. Kim DY, Lee J, Bin, Lee DY, Seo KH (2020) Plasticization effect of poly(lactic acid) in the poly(butylene adipate-co-terephthalate) blown film for tear resistance improvement. Polymers 12:1904. https://doi.org/10.3390/POLYM12091904
75. Luzi F, Torre L, Puglia D (2020) Antioxidant packaging Films based on Ethylene Vinyl Alcohol Copolymer (EVOH) and caffeic acid. Molecules 25. https://doi.org/10.3390/molecules25173953